Available online at www.sciencedirect.com
SCIENCE DIRECT®
Thermochimica Acta 429 (2005) 171–178
thermochimica acta
www.elsevier.com/locate/tca

Nonisothermal crystallization and melting behavior of mPE/LLDPE/LDPE ternary blends

Mingtao Run *, Jungang Gao, Zhiting Li

Department of Polymer Science, College of Chemistry and Environmental Science, Hebei University, Baoding 071002, PR China

Received 15 September 2004; received in revised form 4 March 2005; accepted 7 March 2005
Available online 12 April 2005

Abstract

Nonisothermal crystallization kinetics of ternary blends of the metallocence polyethylene (mPE), low-density polyethylene (LDPE) and linear low-density polyethylene (LLDPE) were studied using DSC at various scanning rates. The Ozawa theory and a method developed by Mo were employed to describe the nonisothermal crystallization process of the two selected ternary blends. The results speak that Mo method is successful in describing the nonisothermal crystallization process of mPE/LLDPE/LDPE ternary blends, while Ozawa theory is not accurate to interpret the whole process of nonisothermal crystallization. Each ternary blend in this study shows different crystallization and melting behavior due to its different mPE content. The crystallinity of the ternary blends rises with increasing mPE content, and mPE improve the crystallization of the blends at low temperature. The crystallization activation energy of the five ternary blends that had been calculated from Vyazovkin method was increased with mPE content, indicating that the more mPE in the blends, the easier the nucleus or microcrystallites form at the primary stage of nonisothermal crystallization. LLDPE and mPE may form mixed crystals due to none separated-peaks were observed around the main melting or crystallization peak when the ternary blends were heating or cooling. The fixed small content of LDPE made little influence on the main crystallization behavior of the ternary blends and the crystallization behavior was mainly determined by the content of mPE and LLDPE.

Keywords: Metallocence polyethylene; Low-density polyethylene; Linear low-density polyethylene; Nonisothermal crystallization kinetics; Ternary blends

1. Introduction

Global consumption of metallocence polyethylene (mPE) resins has been virtually doubling every year since their commercialization in 1995 [1]. Due to its specific properties, such as high mechanical and chemical resistance, puncturable-resistance, transparence, etc., mPE has been widely used as film, molding products although its cost is higher than the traditional polyethylene [2]. On the other hand, the poor melt strength and high melting temperature cause it difficult to processing mPE melt into high quality product due to its narrow MWD and narrow component distribution [3,4], so that some traditional polyethylene as we have known, such as LDPE and LLDPE, are used to not only improve the rheology properties of mPE but also lower the cost of the final product [5,6]. In recent years, the world has shifted strongly towards mPE blends with traditional polyethylene in its application as food or non-food packaging film. As a result, the research in rheology and morphology of the blends of mPE with traditional PE has attracted a good deal of attention for a long time [7–15]. Some studies focus on the crystallization kinetics of the binary blends [8–11], while others attempt to delineate the conditions under which phase separation in the melt will occur [12–15]. In general these studies indicate that branched polyethylenes improve the rheology or processing ability of mPE, and phase separation may be found in the melt depended on the molecular weight of the components and the ratio of linear content to the branched component. In the former research [5,16], a small content (<20 wt.%) LDPE will improve the rheology but lose little mechanical strength of the mPE/LDPE blends, and the crystallization

* Corresponding author.
E-mail address: rmthyp@hotmail.com (M. Run).

0040-6031/$ – see front matter © 2005 Elsevier B.V. All rights reserved.
doi:10.1016/j.tca.2005.03.007

behavior of blends is determined mainly by the mPE component.

Investigations of the kinetics of polymer crystallization are significant both theoretically and practically. Polymers usually undergo a nonisothermal crystallization process in product processing; therefore, a study on the nonisothermal crystallization process of mPE/LLDPE/LDPE blends is meaningful. However, so far, there is no report on the nonisothermal crystallization behaviors of mPE/LLDPE/LDPE ternary blends.

In this study the Ozawa theory and a method developed by Mo were employed to describe the nonisothermal crystallization process of the mPE/LLDPE/LDPE blends at various cooling rates, and an advanced integral isoconversional method developed by Vyazovkin was used to calculate the activation energy of crystallization.

2. Theoretical background

The relative crystallinity ($X_c(t)$) as a function of temperature is defined as the following equation:

$$X_c(t) = \frac{\int_{t_0}^{t} (dH_c/dt)\,dt}{\int_{t_0}^{t_\infty} (dH_c/dt)\,dt} = \frac{A_0}{A_\infty} \tag{1}$$

where t_0 and t_∞ are the time at which crystallization starts and ends, and A_0 and A_∞ the areas under the normalized DSC curves.

The absolute crystallinity (X_c) is defined as:

$$X_c = \frac{\Delta H_f}{\Delta H_f^\circ} \times 100 \tag{2}$$

where ΔH_f and ΔH_f° are the melting enthalpies of sample and 100% crystallization sample (ca. $\Delta H_f^\circ = 279\,J/g$ [13]), respectively. ΔH_f is acquired by the integral area of a DSC heating curve, and the absolute crystallinity, X_c, is a decreasing function of the cooling rate. The half-time of crystallization ($t_{1/2}$) is the required time for 50% crystallization. Generally, the smaller the value of $t_{1/2}$, the faster the crystallization rate is.

2.1. The Ozawa theory [17]

The Avrami theory [18] has been widely used for the interpretation of the isothermal crystallization process:

$$1 - X_c(t) = \exp(-Z_t t^n) \tag{3}$$

$$\log[-\ln(1 - X_c(t))] = n \log t + \log(-Z_t) \tag{4}$$

where $X_c(t)$ is the relative degree of crystallinity at time t; the exponent n is a mechanism constant with a value depending on the type of nucleation and the growth dimension, and the parameter Z_t is a growth rate constant involving both nucleation and growth rate parameters.

Ozawa extended the Avrami equation to the nonisothermal condition. Assuming that the nonisothermal crystallization process may be composed of infinitesimally small isothermal crystallization steps, the following equation was derived:

$$1 - X_c(T) = \exp\left[-\frac{K(T)}{|D|^m}\right] \tag{5}$$

$$\log[-\ln(1 - X_c(T))] = \log K(T) - m \log D \tag{6}$$

where D is the cooling rate, $K(T)$ a function related to the overall crystallization rate that indicates how fast crystallization proceeds, and m the Ozawa exponent that depends on the dimension of crystal growth. According to Ozawa's theory, the relative crystallinity, $X_c(T)$, can be calculated from these equations. By drawing the plot of $\log[-\ln(1 - X_c(T))]$ versus $\log D$ at a given temperature, we should obtain a series of straight lines if the Ozawa analysis is valid, and the kinetic parameters m and $K(T)$ can be derived from the slope and the intercept, respectively.

2.2. The theory of Mo [19]

Mo et al. proposed a different kinetic equation by combining the Avrami and Ozawa equations. As the degree of crystallinity was related to the cooling rate D and the crystallization time t (or T), the relationship between D and t could be defined for a given degree of crystallinity. Consequently, a new kinetic equation for nonisothermal crystallization was derived by combining Eqs. (4) and (6):

$$\log Z_t + n \log t = \log K(T) - m \log D \tag{7}$$

$$\log D = \log F(T) - b \log t \tag{8}$$

where the parameter $F(T) = [K(T)/Z_t]^{1/m}$, the Avrami exponent n is calculated using Ozawa's method, and b the ratio between the Avrami and Ozawa exponents, i.e. $b = n/m$. $F(T)$ refers to the value of cooling rate chosen at unit crystallization time when the system amounted to a certain degree of crystallinity. The smaller the value of $F(T)$ is, the higher the crystallization rate becomes. Therefore, $F(T)$ has a definite physical and practical meaning.

3. Experimental

3.1. Materials and blends preparation

The sample mPE (D60) is supplied by Exxon Co.; LDPE (0274) and LLDPE (218W) are supplied by Qatar PE trochemical Co. Ltd. All samples are in sheet form and their physical characteristics are listed in Table 1.

The weight percentage of LDPE in ternary blends is usually set as 20% in products, so in this research the weight percentage of each component in mPE/LLDPE/LDPE blends are set as B1: 0/80/20; B2: 16/64/20; B3: 32/48/20; B4: 48/32/20; B5: 64/16/20, respectively. The blends with various compo-

nents are put into a Haake Rheomix internal mixer and then the melting compounding is performed at 160 °C for 10 min; the rotor speed is 60 rpm and the total mixing weight per batch was 80 g.

3.2. Differential scanning calorimetry (DSC)

Nonisothermal crystallization behaviors of the ternary blends are studied using a Perkin-Elmer DSC-7 and the weights of all samples are approximately 6 mg. The DSC is calibrated with indium prior to performing the experiment. The samples are heated to 180 °C at a heating rate of 80 °C/min under a nitrogen atmosphere and held for 5 min to remove previous thermal history. Nonisothermal crystallization kinetics is investigated by cooling these samples from 180 to 25 °C at constant cooling rates of 2.5, 5, 10, 15, 20, 25 °C/min. These samples are first cooling from 180 to 25 °C at constant cooling rate of 80 °C/min and then heated them to 180 °C at a heating rate of 10 °C/min to record the melting behavior.

4. Results and discussion

4.1. Crystallization behavior of the ternary blends

Much of the work has been focused on the structure-crystallization property relations for different degree or type of branching polyethylene [8–11,20–25]. It is generally believed that the more and the longer the branched-chain, the lower the crystallization temperature is. The commercial products LDPE, LLDPE and mPE have different structure of molecular chains. The LDPE contains some short-chain branches as well as a few long-chain branches and a much wider MWD. The LLDPE has a narrow MWD and more homogenous side branch length, typically with no long-chain branches; while mPE has a much narrow MWD and linear molecular chains with a few even-distributed short-chain branches. The melt-crystallization curves of the plain mPE, LLDPE and LDPE at the same cooling rate are shown in Fig. 1, and their physical parameters are listed in Table 1. The plain mPE show a higher crystallization temperature T_{onset} = 110.5 °C than that of LLDPE and LDPE (109.5 and 101.3 °C, respectively). When the melt is cooled to room temperature at a given cooling rate, mPE and LLDPE show the same crystallization peak temperature (T_p) at about 108 °C, but the DSC analysis of mPE reveals two steps in the crystallization process: a major and sharper exotherm at higher temperature, and a broader and weaker transition from 100 to 80–90 °C. The pronounced peak at 108 °C is attributed to the crystalline phase of long linear segments in mPE and the unconspicuous peak at about 97 °C is attributed to the crystalline fraction of short-branched chains in mPE [25]. Plain LDPE has a much lower T_p at about 97.8 °C. The reason

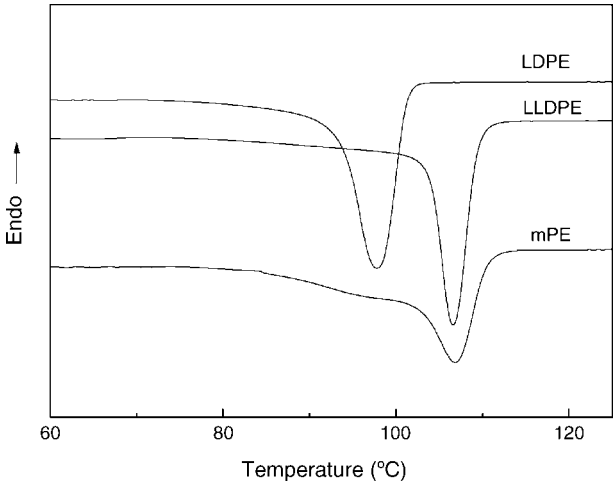

Fig. 1. DSC crystallization curves of pure mPE, LLDPE and LDPE at the cooling rate of 10 °C/min.

Table 1
Physical properties of mPE, LLDPE and LDPE

Sample	Density[a] (g/cm^3)	$MI_{190/2160}$[a] (g/10 min)	M_w[b]	M_w/M_n	Branch degree[b]	Melt point (°C)
mPE	0.942	0.8	100700	2.3	16	122
LLDPE	0.939	1.3	101600	3.6	36	122
LDPE	0.925	1.7	113200	11.0	49	114

[a] Measured by μPRZ-400 FRI.
[b] Obtained from supplier.

Table 2
Parameters of B1 blends during nonisothermal crystallization process

D (°C/min)	B1					B4				
	T_{onset} (°C)	T_{p1} (°C)	t_c (s)	$t_{1/2}$ (s)	X_c (%)	T_{onset} (°C)	T_{p1} (°C)	t_c (s)	$t_{1/2}$ (s)	X_c (%)
2.5	115	113	1962	468	44.5	116	113	2034	502	45.1
5	113	111	938	222	42.4	114	111	942	233	42.9
10	111	109	444	93	40.7	112	108	467	112	42.7
15	110	107	271	57	39.3	110	106	279	74	42.1
20	109	106	191	48	39.0	109	105	200	58	41.6
25	109	105	144	39	38.3	108	104	145	43	39.7

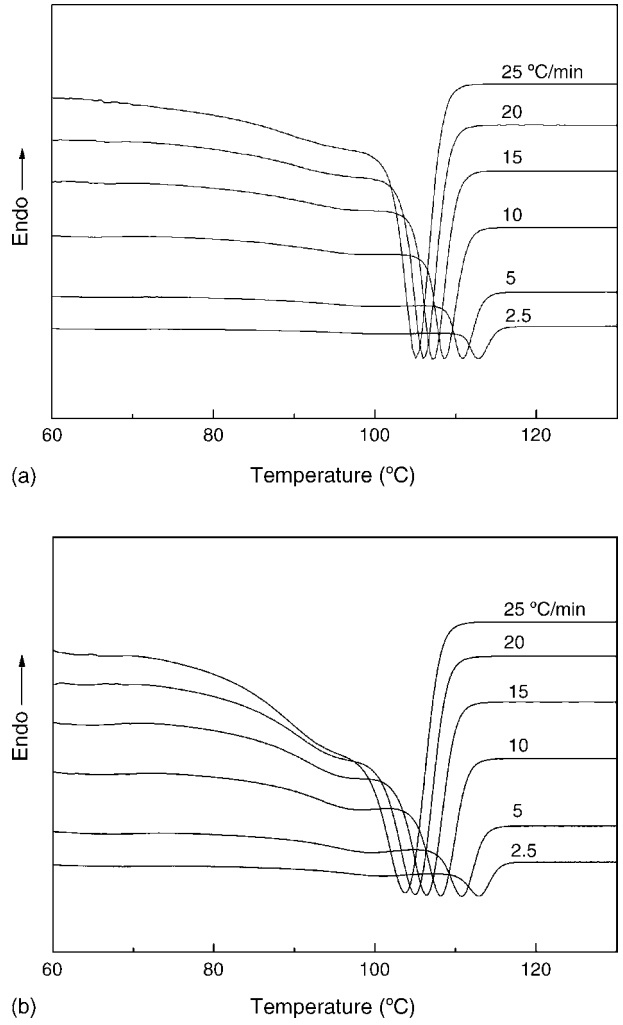

Fig. 2. DSC crystallization curves of (a) B1 and (b) B4 samples at various cooling rates.

for this is that the long branch-chains in LDPE intertwine together to form many tied points which lead to a slower arraying of the molecular chains into folded state in the cooling process.

Fig. 2(a) and (b) shows the crystallization behavior of B1 and B4 blends with different mPE content. The DSC parameters of B1 and B4 at various cooling rates are listed in Table 2. For both B1 and B4, it is seen that the lower the cooling rate, the earlier the crystallization starts; therefore, T_p and T_{onset} shift to lower temperature, which is attributed to the lower time scale that allows the polymer to crystallize with increasing cooling rate, thus requiring a higher supercooling to initiate crystallization. When the specimens are cooled fast, the motion of the PE molecular chains is not able to follow the cooling temperature. Furthermore, t_c and $t_{1/2}$ are gradually decreased with increasing cooling rate for both B1 and B4, indicating a higher cooling rate, a faster crystallization rate. Meanwhile, the absolute crystallinity is gradually decreased with increasing cooling rate for both B1 and B4, but the X_c value of B4 is slightly bigger than that of B1, indicating that a higher crystallization ability of ternary blend with more content of mPE.

In Fig. 2(a), for all the cooling rates, the DSC curves display two exotherms: a sharp peak at high temperature, and a broader transition at lower temperature, which is more evident at high cooling rates. According to the temperature data of the plain LDPE and LLDPE in Fig. 1, the sharp peak at high temperature is attributed to the crystalline phase of LLDPE and the broader transition at lower temperatures is attributed to the crystalline fraction of LDPE. While in Fig. 2(b), the exotherms at low temperature is only sharper, and there are no changes in temperature. In the DSC curves of B4, the sharp peak at high temperatures is attributed to the crystalline phase of LLDPE and the long linear segments in mPE, while the broader transition at lower temperatures is attributed to the crystalline fraction of LDPE and the short-branched chains in mPE. These results indicating that mPE increase the crystallization of blends at low temperature. This result is also can be observed in Fig. 3, the DSC curves of blends with various mPE content at a given cooling rate. It is clearly that the crystallization peaks at lower temperature become sharper with increasing mPE content; however, no separate peaks is observed around 110 °C because mPE and LLDPE have nearly the same crystallization peak temperature and some mixed crystals might be formed in the ternary blends.

From DSC crystallization curves of the blends, the relative crystallinity as a function of temperature for ternary blends is shown in Fig. 4(a) and (b). It can be seen that all these curves have similar sigmoidal shape, and the curvature of the upper part plot is observed to be level off due to the spherulite impingement or crowding in the final stage of crystallization. In this case, the values of t_c and $t_{1/2}$ are increased with increasing mPE content (Table 2). These results indicate an increase of the whole crystallization time with increasing mPE content and mPE improves the crystallization ability of the blends at low temperature that is much below the maximum crystallization peak temperature.

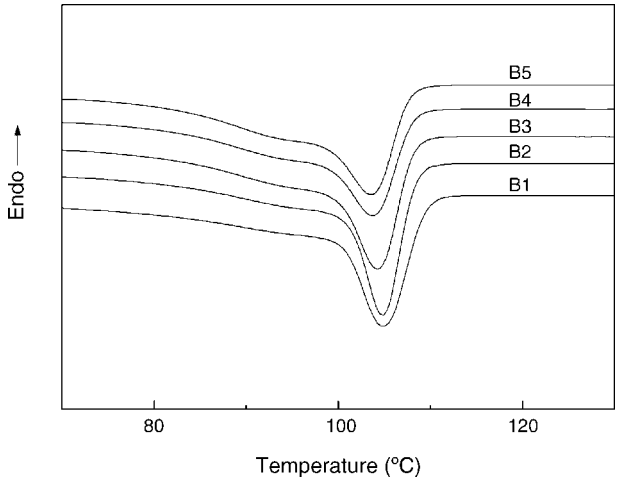

Fig. 3. DSC crystallization curves of five ternary blends at the cooling rate of 25 °C/min.

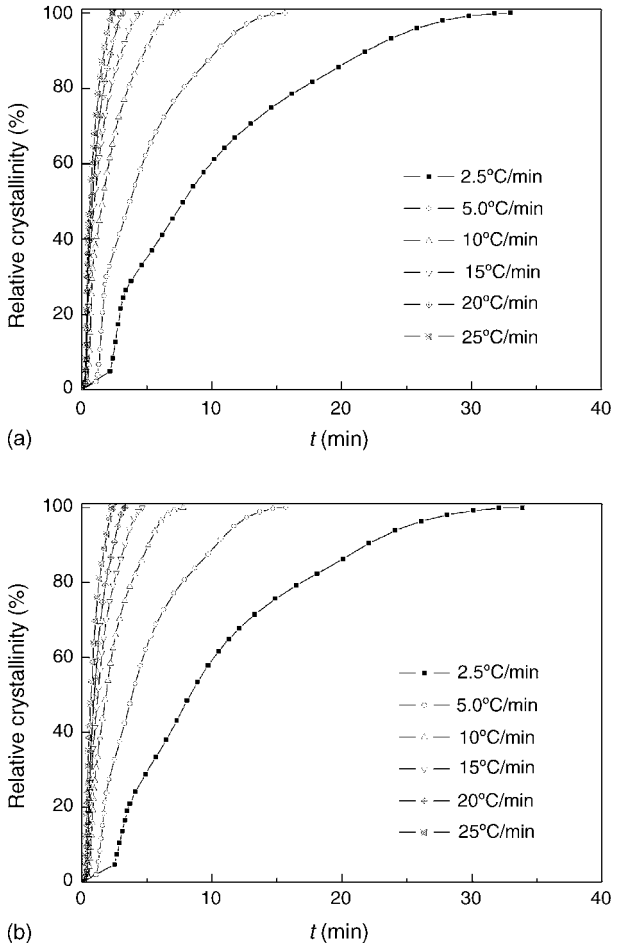

Fig. 4. Relative crystallinity vs. time for nonisothermal crystallization of (a) B1 and (b) B4 samples.

4.2. Melting curves of ternary blends

Fig. 5 shows a series of DSC thermograms of different ternary blends at a heating rate of 10 °C/min and the parameters are listed in Table 3. It is clearly seen from Fig. 5 and Table 3 that all endotherms exhibit two main melting peaks: a major and sharper peak at higher temperature (T_{m1}), and a broader and unconspicuous peak at lower temperature (T_{m2}). These two peaks all shift to higher temperature with increasing mPE content. At this heating rate, the broader peak may be contains the melting of small content LDPE crystals, big content LLDPE and mPE crystals formed at low temperature, therefore, its intensity increases with increasing mPE content. There is only one peak observed in the sharper melting peak at high temperature, which indicating that the mixed crystals have been formed by mPE and LLDPE. The melting enthalpy and crystallinity also rise with increasing mPE content due to mPE's high crystallization ability.

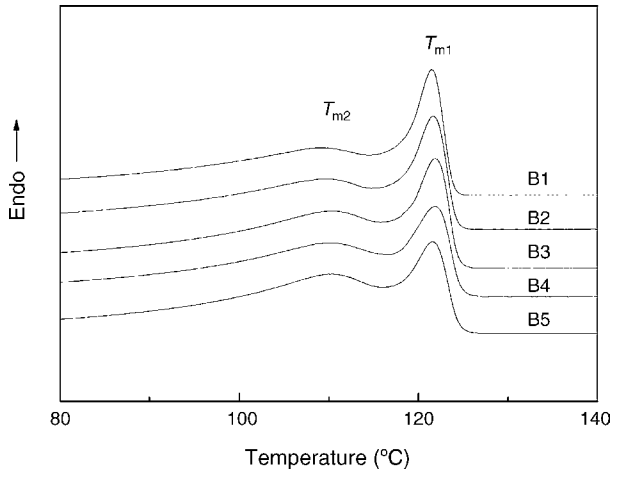

Fig. 5. DSC melting thermograms of five ternary blends at the heating rate of 10 °C/min.

Table 3
Parameters of series ternary blends during the heating rate of 10 °C/min

Sample	T_{m1} (°C)	T_{m2} (°C)	ΔH_f (J/g)	X_c (%)
B1	121	109	126.4	45.3
B2	122	110	128.5	46.1
B3	122	110	129.7	46.5
B4	122	110	131.4	47.1
B5	122	110	133.6	47.9

4.3. Nonisothermal crystallization kinetics

According to Ozawa's theory and plots of $\log[-\ln(1-X_t)]$ versus $\log D$ at a given temperature, we should obtain a series of straight lines if Ozawa analysis is valid, and the kinetic parameters m and $K(T)$ can be derived from the slope and the intercept, respectively. The results of Ozawa analysis for B1 and B4 blends are shown in Fig. 6(a) and (b). All lines are not straight with the change of cooling rate especially at the high cooling rate above 20 °C/min, and the curvature of the plots increases with the cooling rate. On the other hand, the curvatures of the lines show different tendency at different temperature, in which the higher the temperature is, the more the curvature.

Therefore, the accurate analysis of nonisothermal crystallization data could not be performed because the variation in the slope with temperature. It means that the parameter m is not a constant during crystallization and that Ozawa's approach is not suitable to describe the nonisothermal crystallization process for the ternary blends. Sajkiewicz et al. [26] report that the linear function as predicted by Ozawa is observed only for data obtained at relatively low cooling rates below 20 °C/min. The increased cooling rate causes a decrease of absolute crystallinity and an increase of the fraction of amorphous phase between spherulites (Table 2). In this research, it is the cooling rate above 20 °C/min that causes the curvature increased much with cooling rate, especially at high temperature. This can be explained that, at a given temperature, the crystallization process at different cooling rate are at

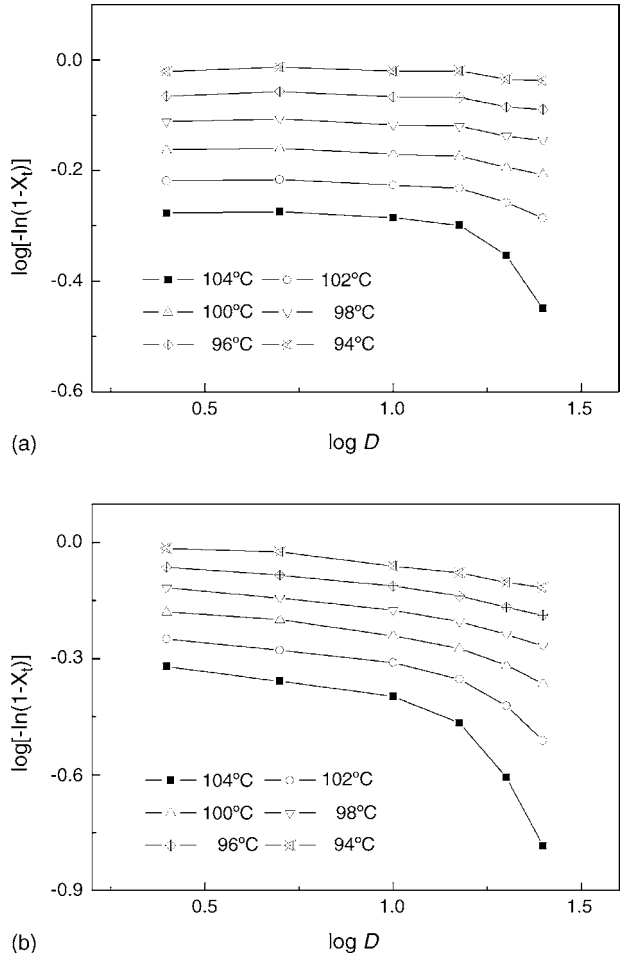

Fig. 6. Ozawa plots of $\log[-\ln(1-X_t)]$ vs. $\log D$ for nonisothermal crystallization of (a) B1 and (b) B4 samples.

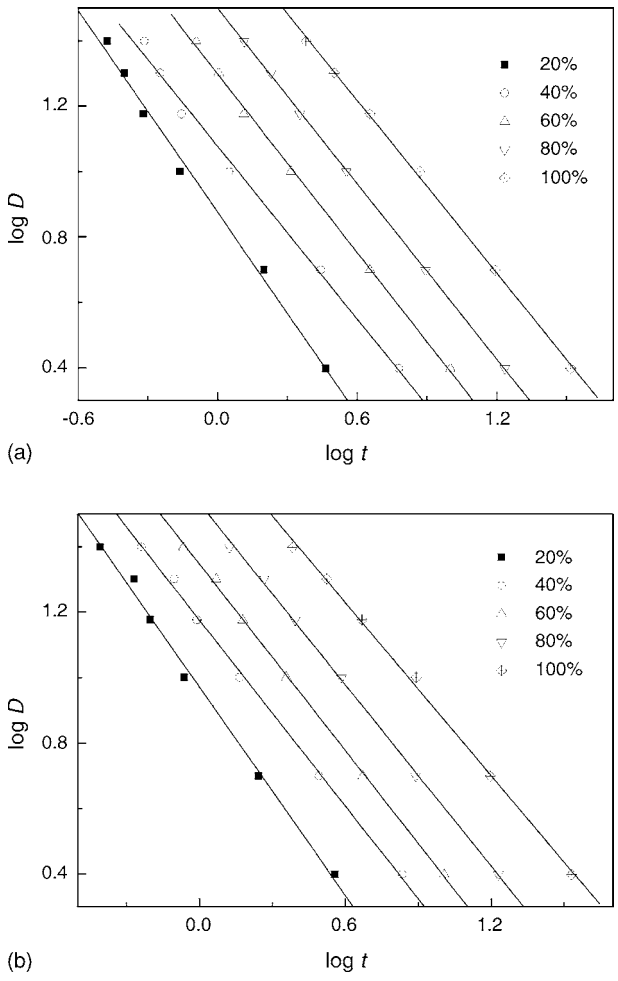

Fig. 7. Log D vs. log t from the Mo equation for (a) B1 and (b) B4 samples.

different stages; that is, the lower cooling rate process is toward the end of crystallization process, whereas at the higher cooling rate, crystallization process is at an early stage.

The method developed by Mo is also employed to describe the nonisothermal crystallization. At a given crystallinity, the plot of log D against log t will give a straight line with an intercept of log $F(T)$ and a slope of $-b$. As shown in Fig. 7(a) and (b), plotting log D against log t of both B1 and B4 demonstrates linear relationship at a given X_t, and the values of $F(T)$ and b are listed in Table 4. To each blend, $F(T)$ values are increased with the relative crystallinity, indicating a lower crystallization rate is needed to reach the given crystallinity within unit time. At a given X_t, $F(T)$ values rise slightly with increasing mPE content, indicating the more the mPE content, the lower the crystallization rate is. The parameter b is decreased with increasing X_t. Thus, these equations of Mo method successfully describe the nonisothermal crystallization process of the ternary blends on the whole crystallization process.

Table 4
Nonisothermal crystallization parameters of blends at each given relative crystallinity

X_t (%)	20	40	60	80	100
B1					
b	1.03	0.92	0.91	0.89	0.88
log $F(t)$	0.88	1.08	1.30	1.50	1.75
B2					
b	1.05	0.97	0.96	0.97	0.93
log $F(t)$	0.91	1.11	1.32	1.53	1.78
B3					
b	1.0	0.94	0.93	0.92	0.91
log $F(t)$	0.94	1.13	1.31	1.50	1.77
B4					
b	1.06	0.95	0.95	0.92	0.88
log $F(t)$	0.97	1.18	1.35	1.53	1.76
B5					
b	1.06	0.95	0.94	0.92	0.87
log $F(t)$	0.96	1.17	1.34	1.52	1.75

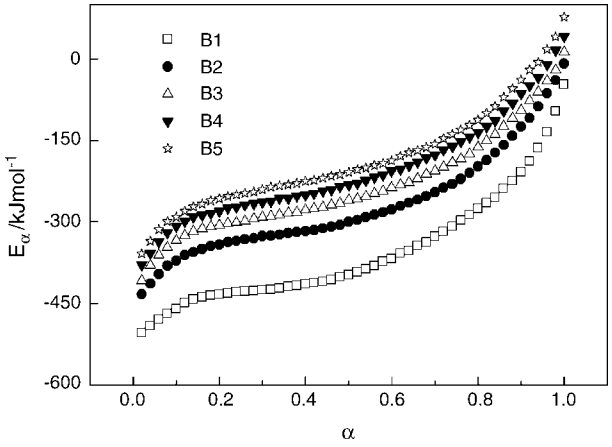

Fig. 8. Dependence of the activation energy on the crystallization conversion extent of five ternary blends.

4.4. Crystallization activation energy

In order to obtain the reliable values of the effective activation energy on the melt-cooling process, an advanced isoconversional method developed by Vyazovkin [27–29] has been used to evaluate the effective activation energies as shown in Eq. (9):

$$\Phi(E_\mathrm{a}) = \sum_{i=1}^{n} \sum_{j\neq i}^{n} \frac{J[E_\mathrm{a}, T_i(t_a)]}{J[E_\mathrm{a}, T_j(t_a)]} \tag{9}$$

where

$$J[E_\mathrm{a}, T_i(t_a)] \equiv \int_{t_a-\Delta a}^{t_a} \exp\left[\frac{-E_\mathrm{a}}{RT_i(t)}\right] \mathrm{d}t \tag{10}$$

In Eq. (10) a varies from a to $1-\Delta a$ with a step $\Delta a = m^{-1}$, where m is the number of intervals chosen for analysis and it is set as $m = 50$ in this calculation. Fig. 8 shows the dependence of the activation energy on the extent of crystallization conversion of five blends. To each blend, the activation energy increases with the extent of the melt conversion, e.g. the activation energy increases from −504 to −40 kJ/mol for sample B1, while it rises from −358 to 67 kJ/mol for sample B5. By comparing the activation energy at the same extent of melt conversion, e.g. $a = 0.4$, their values are −412 kJ/mol (B1), −313 kJ/mol (B2), −279 kJ/mol (B3), −249 kJ/mol (B4) and −225 kJ/mol (B5), respectively. The mPE has much long linear segments in its molecular chains, and they can nucleate and crystallize easily in blends than LLDPE, that is, the more mPE content, the more nucleus or microcrystallites form in blend. Therefore, mPE improve the crystallization ability of the blend.

5. Conclusions

The Ozawa analysis fails to provide an adequate description of nonisothermal crystallization of mPE/LLDPE/LDPE due to the deviation of plots especially at high cooling rates and high temperature. While the theory developed by Mo is successful in describing the nonisothermal crystallization process of mPE/LLDPE/LDPE blends. The crystallization peaks of the ternary blends become broader toward low crystallization temperature with increasing mPE content, and no separated-peaks is observed around 110 °C for mPE and LLDPE may form into mixed crystals in the ternary blends. The fixed small content of LDPE made little influence on the predominant crystallization behavior of the blends, thus the crystallization behavior of the ternary blends is mainly determined by the content ratio of mPE to LLDPE. From the results of activation energies of series ternary blends determined by Vyazovkin method, it can be seen that the crystallization activation energy of the blends rises with increasing mPE content, which indicating that the mPE improve the crystallization ability of the blend.

In this research, however, the increasing of the mPE content in ternary blends does not cause sharp change in various parameters of DSC curves due to the similarity of chemical component of the three polymers possessing with only different branch degree of molecular chains. But it is meaningful to provide some information about the crystallization or melting behaviors of the blends with various mPE components for their widely using in industrial application.

Acknowledgments

This work is supported by the financial support from the Natural Science Foundation (No. 201068) and Educational Science Foundation (No. 2000105) of Hebei Province, PR China.

References

[1] Asia/Pacific becomes leading polyethylene consumer, Plastics Addit. Compd. 5 (2003) 10.
[2] R.B. Howard, Single-site materials redefining the polymer industry, in: Proceedings of the Metcon'97 on Polymers in Transition, Houston, TX, USA, 1997, pp. 4–5.
[3] J.F. Vega, A. Munoz-Escalona, A. Santanaria, et al., Macromolecules 29 (1996) 960.
[4] Y.S. Kim, C.I. Chung, S.Y. Lai, et al., J. Appl. Polym. Sci. 59 (1996) 125.
[5] M.T. Run, J.G. Gao, Z.T. Li, China Plastic Ind. 29 (2001) 37.
[6] M.T. Run, J.G. Gao, Z.T. Li, China Polym. Mater. Sci. Eng. 19 (2003) 175.
[7] G.H. Fredrickson, A.J. Liu, F.S. Bates, Macromolecules 27 (1994) 2503.
[8] J.G. Gao, M.S. Yu, Y.F. Li, et al., J. Appl. Polym. Sci. 89 (2003) 2431.
[9] C.C. Puig, Polymer 42 (2001) 6579.
[10] R.S. Stein, S.R. Hu, T.J. Kyu, J. Polym. Sci., Polym. Phys. 25 (1987) 27.
[11] D. Norton, A. Keller, J. Mater. Sci. 19 (1984) 447.
[12] M.J. Hill, P.J. Barham, Polymer 38 (1997) 5595.
[13] R.G. Alamo, W.W. Graessley, R. Krishnamoorti, et al., Macromolecules 30 (1997) 561.
[14] B.S. Tanem, A. Stori, Polymer 42 (2001) 4309.

[15] B.S. Tanem, A. Stori, Thermochem. Acta 345 (2001) 73.
[16] M.T. Run, J.G. Gao, Y.F. Liu, et al., J. Hebei Univ. 21 (2001) 277.
[17] T. Ozawa, Polymer 12 (1971) 150.
[18] M. Avarami, J. Chem. Phys. 7 (1939) 1103.
[19] T. Liu, Z. Mo, S. Wang, et al., Polym. Eng. Sci. 37 (1997) 568.
[20] P. Galli, J.C. Haylock, G.C. Rollefson, et al., Proceedings of the Metallocene Technology'97, Chicago, IL, 1997.
[21] E.T. Hsieh, C.C. Tso, J.D. Byers, et al., J. Macromol. Sci. Phys. B 36 (1997) 615.
[22] S. Hosoda, Polym. J. 20 (1988) 383.
[23] J.T. Xu, Z.Q. Fan, Q. Wang, Acta Polym. Sinica 5 (1997) 624.
[24] G.D. Wignall, R.G. Alamo, J.D. Londono, et al., Macromolecules 33 (2000) 551.
[25] H. Wu, S. Guo, G. Chen, J. Appl. Polym. Sci. 94 (2004) 2522.
[26] P. Sajkiewicz, L. Carpaneto, A. Wasiak, Polymer 42 (2001) 5365.
[27] S. Vyazovkin, J. Comput. Chem. 18 (1997) 393.
[28] S. Vyazovkin, J. Comput. Chem. 22 (2001) 178.
[29] S. Vyazovkin, N. Sbirrazzuoli, Macromol. Rapid Commun. 23 (2002) 766.